Electronic Supplementary Material (ESI) for Dalton Transactions.

Supporting Information

Spectroelectrochemical studies of the redox active tris[4-(triazol-1-yl)phenyl]amine linker and redox state manipulation of Mn(II)/Cu(II) coordination frameworks

Chin-May Ngue,[a,b] Yen-Hsiang Liu,[c] Yuh-Sheng Wen,[a] Man-Kit Leung,*[b,d] Ching-Wen Chiu,*[b] Kuang-Lieh Lu*[a]

[a]Institute of Chemistry, Academia Sinica, Taipei 115, Taiwan

[b]Department of Chemistry, National Taiwan University, Taipei 106, Taiwan

[c]Department of Chemistry, Fu Jen Catholic University, New Taipei City 242, Taiwan

[d]Department of Chemistry, Advanced Research Centre for Green Materials Science and Technology, National Taiwan University, Taipei 106, Taiwan

Solid state *in situ* spectroelectrochemical (UV/Vis/NIR) method

2 to 3 mg of **1** and **2** were lightly ground using a mortar and pestle, respectively. Indium tin oxide (ITO) glass (6 cm x 0.9 cm) was pretreated by washing with ethanol, acetone and purging with nitrogen. **1** and **2** were coated on the ITO glass, by spreading evenly with a spatula. Nafion in the propionitrile solution was carefully layered on top of the solid to serve as a binder. The electrochemical set up employed a three-electrode system with ITO as the working electrode, Pt mesh as the counter electrode and Ag/Ag^{+} as the reference electrode in a 0.1 M *n*-Bu_4NPF_6 propionitrile electrolyte. The three electrochemical cell was placed inside a 1 cm quartz cell, with the coated ITO sample and Pt mesh facing opposite in the cell. To minimize the risk of short-circuits, the compartment was separated by a tailor-made Teflon block. The electrolyte solution served as a baseline. A blank ITO glass was measured as the background value. Samples were scanned continuously with incremental potentials using a Hokuto Denko potentiostat until a change in the spectrum was observed. The spectral was measured by means of a JASCO V-570 UV-Vis-NIR spectrometer.

***Ex situ* chemical oxidation of 1**

Oxidation by bromine. Solid crystals of **1** was placed inside a small vial. The vial was then placed in a beaker containing 3 to 5 drops of bromine with a watch glass on top. Bromine vapour was allowed to diffuse into framework for 30 minutes. Solid **1** changed to orange colour.

Oxidation by iodine. 10 mg of **1** was prepared inside a 2 mL glass vial. The 2 mL glass vial was then transferred to a 20 mL glass vial with iodine crystals inside. Iodine vapour were allowed to slowly diffuse into the framework. Solid **1** changed to dark brown colour.

Oxidation by Ce(IV). Ceric ammonium nitrate was dissolved in water. A few drops of Ce(IV) were transferred to a glass vial containing solid **1**, Ce(IV) was added until the crystals changed to blue colour.

Computation calculation

Geometry was optimized at B3LYP-D3/def2-TZVP. To speed up the calculation, the RICOSX approximation and def2/J auxilliary basis set were used. At the minimum geometry, a TD-DFT calculation at B3LYP-D3/def2-TZVP was performed to predict the electronic spectrum. All calculations were done using the ORCA 4.1.0 suite of programs.[1]

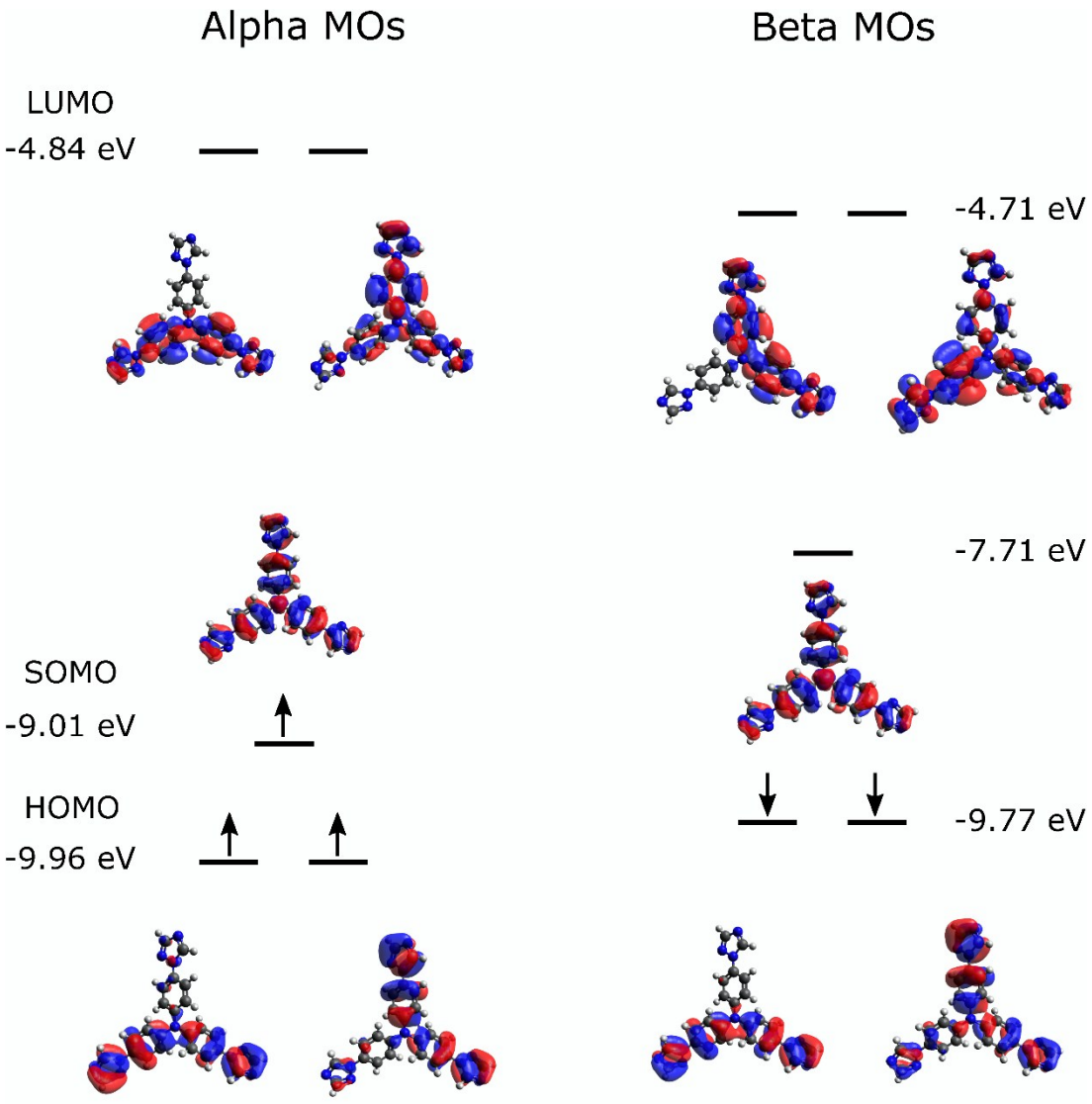

Schematic diagram S1. Unrestricted molecular orbital diagram of TTPA ligand in radical cation state.

Table S1. Crystal data and structure refinement for $[MnCl_2(TTPA)(DMF)]_n$ (**1**).

Empirical formula	$C_{27}H_{25}Cl_2MnN_{11}O$
Formula weight	645.42
Temperature, K	100.0(2)
Wavelength, Å	0.71073
Crystal system	Monoclinic
Space group	*C*2/*c*
a, Å	18.2168(4)
b, Å	15.5104(3)
c, Å	21.1221(5)
β,°	98.252(2)
V, Å^3	5906.3(2)
Z	8
Density (calculated), Mg/m^3	1.452
Absorption coefficient, mm^{-1}	0.671
F(000)	2648
Crystal size, mm^3	0.260 x 0.220 x 0.160
Theta range for data collection, °	1.732 to 27.103
Index ranges	–23<=h<=23, –19<=k<=19, –27<=l<=27
Reflections collected	76708
Independent reflections	6527 [R(int) = 0.0559]
Completeness to theta = 25.000°	100.0 %
Absorption correction	Semi-empirical from equivalents
Refinement method	Full-matrix least-squares on F^2
Data/restraints/parameters	6527/0/381
Goodness-of-fit on F^2	1.038
Final R indices [$I > 2\sigma(I)$]	R1 = 0.0359, wR2 = 0.0852
R indices (all data)	R1 = 0.0498, wR2 = 0.0946

$R_1 = \Sigma||F_0|-|F_c|| / \Sigma|F_0|$; $wR_2 = [\Sigma w(F_0^2-F_c^2)^2 / \Sigma w(F_0^2)^2]^{1/2}$

Table S2. Crystal data and structure refinement details for $[CuCl_2(TTPA)\cdot 1.5DMF]_n$ (**2**).

Empirical formula	$C_{28.5}H_{28.5}Cl_2CuN_{11.5}O_{1.5}$
F_w	690.64
Temperature, K	100.0(2)
Crystal system	Monoclinic
Space group	*C*2/*c*
a, Å	17.7001(7)
b, Å	14.9411(7)
c, Å	22.5015(10)
β, °	96.5309(16)
V, Å^3	5930.1(4)
Z	8
λ, Å	0.71073
D_{calc}, Mg/m^3	1.301
μ, mm^{-1}	0.947
F(000)	2360
Crystal size, mm^3	0.360 × 0.220 × 0.140
Reflections collected	125143
Independent reflections	6562 [R(int) = 0.0802]
Completeness to theta = 25.000°	100.0 %
Absorption correction	Semi-empirical from equivalents
Refinement method	Full-matrix least-squares on F^2
Data/restrains/parameters	6562/0/334
Goodness of fit	1.207
Final R indices [$I > 2\sigma(I)$]	R_1 = 0.0654, wR_2 = 0.1414
R indices (all data)	R_1 = 0.0786, wR_2 = 0.1477

$R_1 = \Sigma||F_0|-|F_c||/\Sigma|F_0|$; $wR_2 = [\Sigma w(F_0^2-F_c^2)^2/\Sigma w(F_0^2)^2]^{1/2}$

Table S3. Selected bond lengths [Å] and angles [°] for **1** and **2**.

1			
Cu(1)–N(4)	1.998(4)	N(4)–Cu(1)–N(7)	175.06(15)
Cu(1)–N(7)	2.003(4)	N(7)–Cu(1)–N(10)	94.03(14)
Cu(1)–N(10)	2.174(4)	N(4)–Cu(1)–Cl(1)	89.31(11)
Cu(1)–Cl(1)	2.3131(13)	N(10)–Cu(1)–Cl(1)	101.59(11)
Cu(1)–Cl(2)	2.3291(12)	Cl(1)–Cu(1)–Cl(2)	156.84(5)
2			
Mn(1)–O(1)	2.2229(15)	O(1)–Mn(1)–N(4)	92.52(6)
Mn(1)–N(9)	2.2659(17)	N(4)–Mn(1)–N(7)	88.57(6)
Mn(1)–Cl(2)	2.4846(6)	N(4)–Mn(1)–N(9)	173.37(6)
Mn(1)–N(4)	2.2254(17)	N(7)–Mn(1)–Cl(2)	95.60(5)
Mn(1)–N(7)	2.2676(17)	O(1)–Mn(1)–N(7)	174.90(6)

Symmetry transformations used to generate equivalent atoms: for **1**: #1 – x + 1, y - 1, – z + 1/2, #2 – x + 1, – y, – z + 1 #3 – x + 1, y + 1, – z + 1/2; for **2**: #1 – x + 1, y – 1, – z + 1/2, #2 x, – y + 1, z + 1/2. #3 – x + 1, y + 1, – z + 1/2, #4 x, – y + 1, z – 1/2

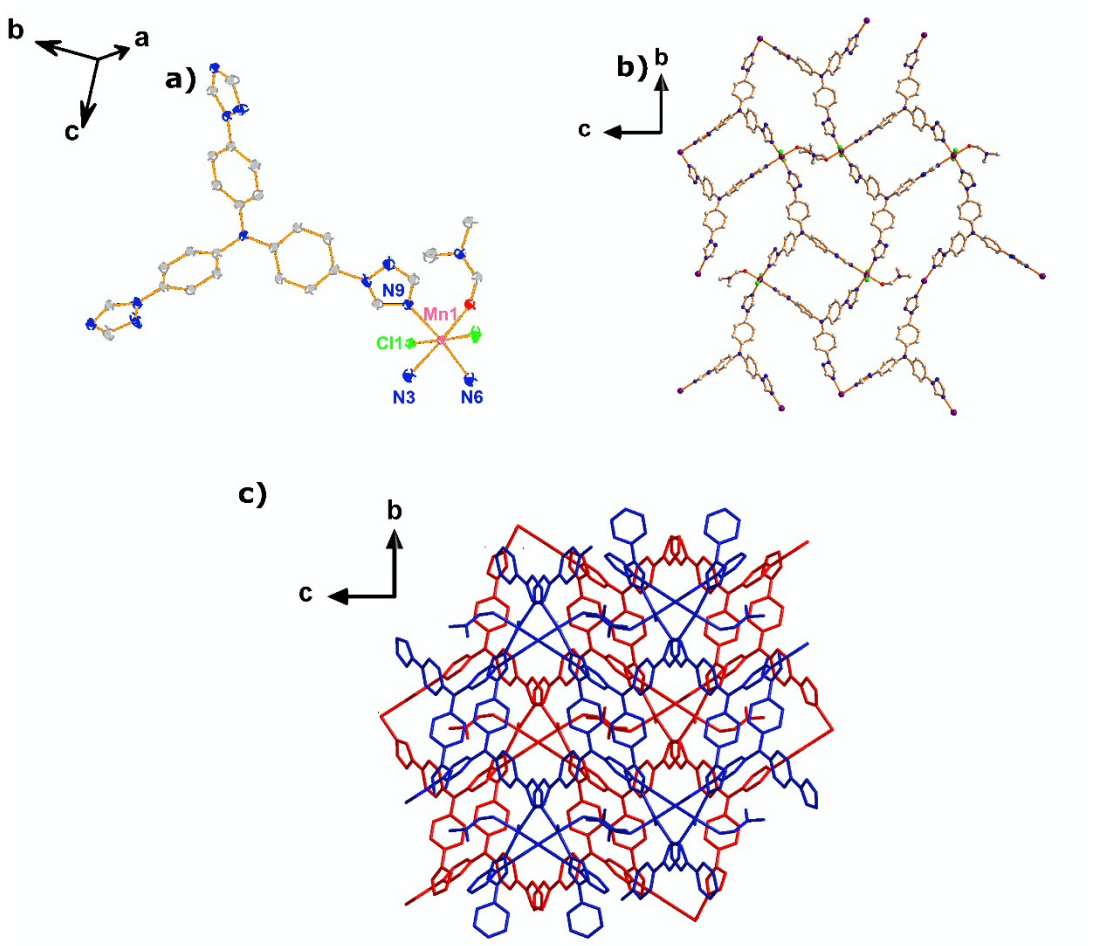

Figure S1. a) Coordination environments of **1**, 50% probability ellipsoids, b) two-dimension view along the *b* axis, c) 2-fold interpenetration of **1** view along the *b* axis.

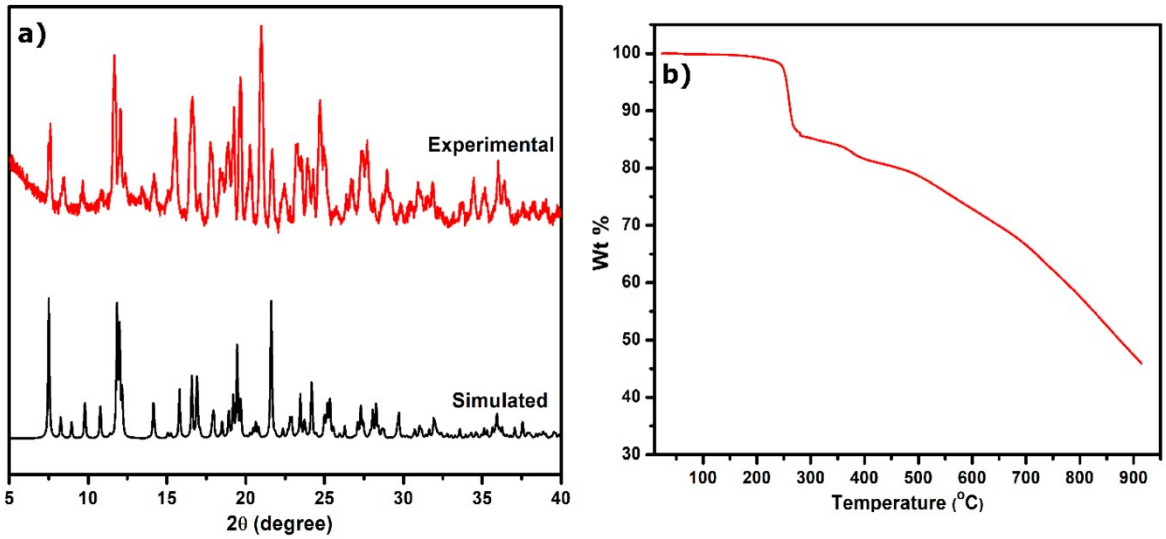

Figure S2. (a) Simulated and experimental PXRD patterns of **1**, (b) thermal gravimetric analysis (TGA) of **1** over the temperature range 30–900 °C.

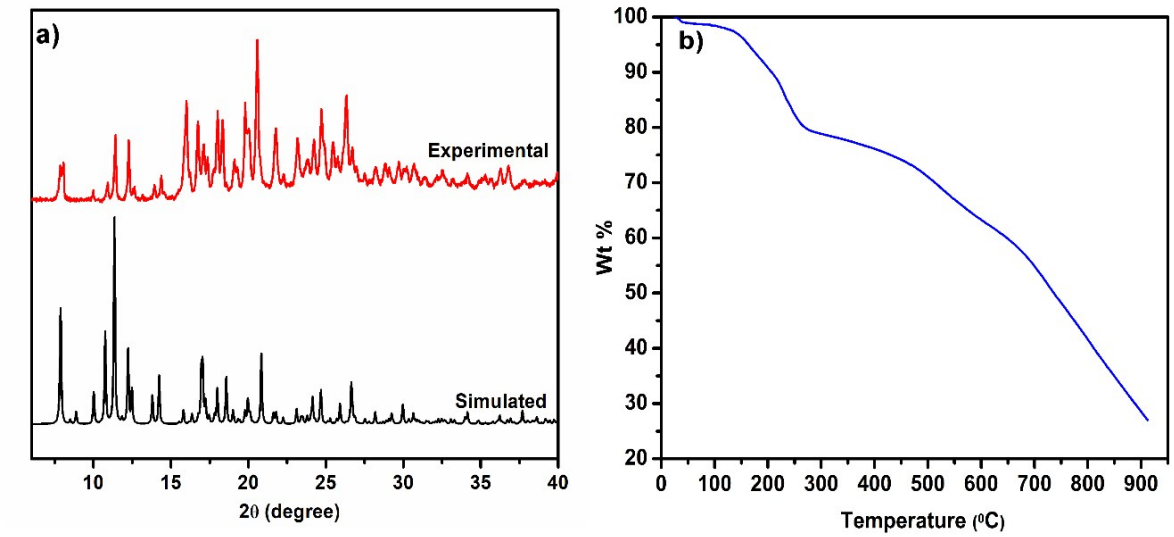

Figure S3. a) Simulated and experimental PXRD patterns of **2**, b) thermal gravimetric analysis (TGA) of **2** over the range 30–900 °C.

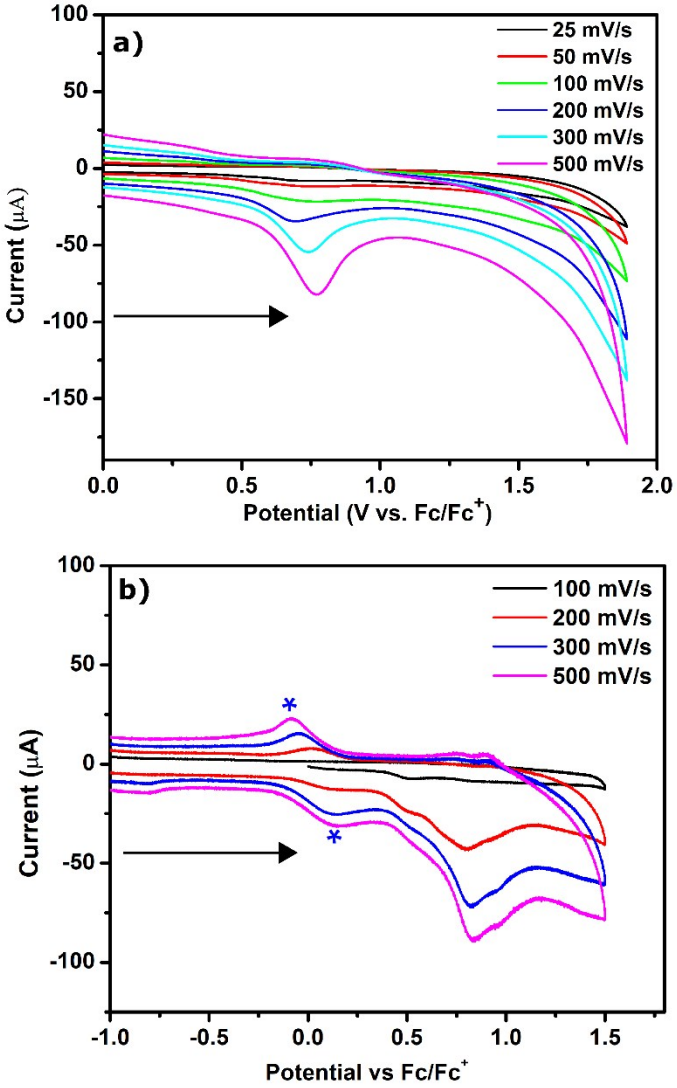

Figure S4. Solid state electrochemistry of **1** (a) and **2** (b) frameworks in 0.1 M [(*n*-$C_4H_9)_4N]PF_6$/propionitrile as the electrolyte over the scan ranges of 25 to 1000 mV/s. The asterisks in Figure 4b represent the added Fc/Fc^+.

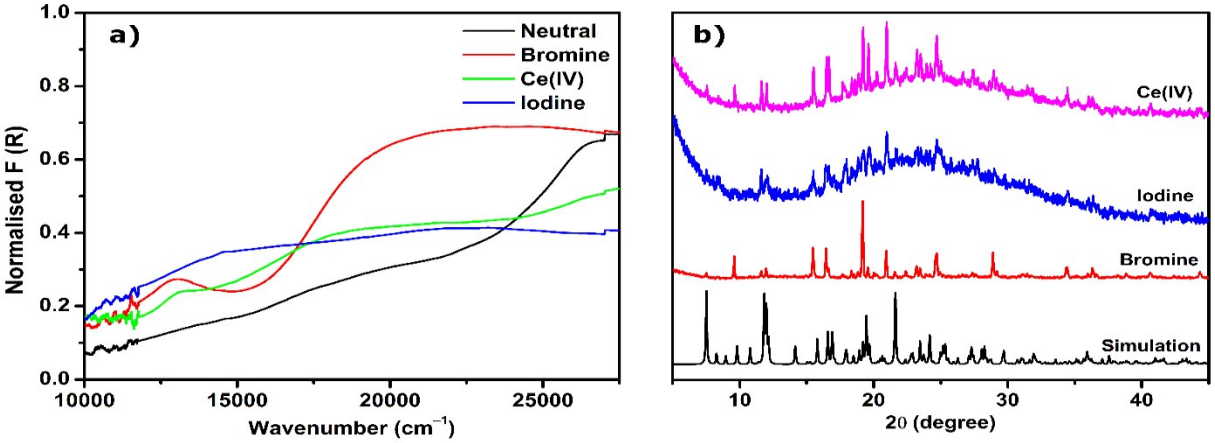

Figure S5. (a) Superimposed UV/Vis/NIR spectra for **1** (neutral) and its oxidised analogues over the range of 10000–45000 cm^{-1}, (b) PXRD patterns of the oxidised analogues.

Reference

1. F. Neese, WIREs *Comput. Mol. Sci.* 2018, 8:e1327. doi: 10.1002/wcms.1327